

RESEARCH

Open Access

Cooperative beamforming for a double-IRS-assisted wireless communication system



Guodong Tian  and Rongfang Song*

* Correspondence: songrf@njupt.edu.cn

The College of Telecommunications and Information Engineering, Nanjing University of Posts and Telecommunications, Nanjing 210003, China

Abstract

Intelligent reflecting surface (IRS) has emerged as an innovative and disruptive solution to boost the spectral and energy efficiency and enlarge the coverage of wireless communication systems. However, the existing literature on IRS mainly concentrates on wireless communication systems assisted by single or multiple distributed IRSs, which are not always effective. In view of this issue, this paper considers a special double-IRS-assisted wireless communication system, where IRS1 and IRS2 are deployed near the base station (BS) and the user, respectively, and the transmitted signals reach the user via the cascaded BS-IRS1-IRS2-user channel only. We cooperatively optimize transmit and passive beamforming on the two IRSs based on the particle swarm optimization (PSO) algorithm to maximize the received signal power. Simulation indicates that despite no direct line-of-sight (LoS) path from the BS to the user, an excellent signal-to-noise ratio (SNR) is available at the receiver with the aid of two IRSs, which demonstrates that it is feasible to assist communication by double reflection links composed of two IRSs. Additionally, we unexpectedly find that when the positions of the two IRSs are fixed, by exchanging the positions of the BS and the user, the obtainable SNRs are similar.

Keywords: Intelligent reflecting surface (IRS), Channel state information (CSI), Beamforming, Particle swarm optimization (PSO)

1 Introduction

Due to its ability to smartly control signal reflection with low-cost passive reflecting elements, intelligent reflecting surface (IRS) (also referred to as reconfigurable intelligent surface (RIS) or large intelligent surface (LIS)) is an innovative and disruptive paradigm that can boost the spectral and energy efficiency and effectively enlarge the coverage of wireless communication systems [1–3]. Furthermore, the reflecting elements are typically made of thin materials, which are light with low power, so IRS can be freely mounted on related objects in the environment to cater to diverse application scenarios. Hence, IRS has attracted great attention from both academia and industry as an enabling technology for future 6G communications [4, 5].

The existing literature on IRS mainly focuses on wireless communication systems assisted by single or multiple distributed IRSs (e.g., [6–10] [11–15]), with each IRS independently serving related users in range through one-time signal reflection. Such an

approach, however, is not always effectual. For instance, due to dense blockages in either indoor or outdoor scenarios, transmitted signals may not be able reach the receivers by means of line-of-sight (LoS) paths and/or blockage-free links directly with only one IRS deployed in the vicinity of the transmitter or receiver. For IRS to play a vital role in the above scenario, two or more IRSs could be exploited to cooperatively serve various terminals with the aid of multihop signal reflection to avoid scattered obstacles.

Inspired by this, this paper proposes a wireless communication system cooperatively assisted by two IRSs, as shown in Fig. 1. Here, we assume that signals reach the receiver via double reflection links, namely, the BS-IRS1-IRS2-user link, while other links are not available because of severe obstacles. Simultaneously, we reasonably and subtly deploy two distributed IRSs in the proximity of the BS and the user (IRS1 and IRS2 are mounted on Building A and Building B, respectively) to achieve LoS channels from the BS to IRS1, IRS1 to IRS2, and IRS2 to the user. It is assumed that the channel state information (CSI) is acquirable. To maximize the received signal power, we employ the particle swarm optimization (PSO) algorithm to cooperatively optimize the transmit beamforming and the phase shifts on two IRSs subject to the maximum transmit power constraint at the BS. The simulation results show that the performance of the wireless communication system can be guaranteed as soon as two IRSs are appropriately deployed near the BS and the user, despite the lack of a direct LoS path being attainable. This demonstrates that it is practicable to improve the quality of wireless communication by double reflection links consisting of two IRSs. In addition, the numerical results indicate that the obtainable SNRs at the receiver are nearly equal by exchanging the positions of the BS and the user when the positions of IRS1 and IRS2 are fixed.

The remainder of this paper is arranged as follows: the system model and problem formulation for double-IRS-assisted wireless communication are presented in Section 2. In Section 3, we adopt the PSO algorithm to address the formulated problem. The simulation results are discussed in Section 4. The conclusions are drawn in Section 5.

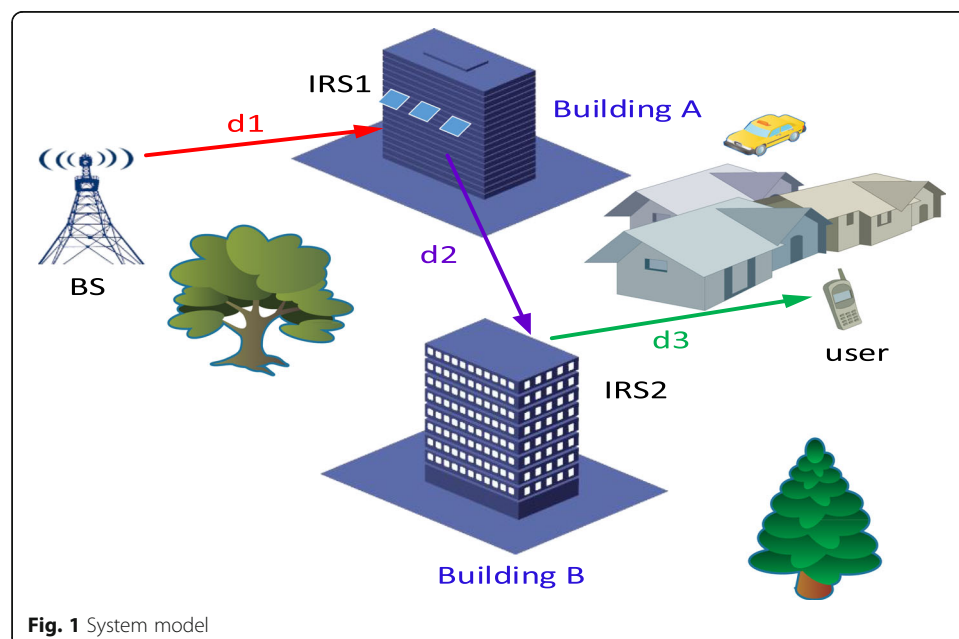


Fig. 1 System model

2 System model and problem formulation

2.1 System model

In this paper, we contemplate an equivalent multiple-input-single-output (MISO) downlink wireless communication system enabled by two distributed IRSs, as shown in Fig. 1, where the BS, IRS1, IRS2, and user are equipped with an M -element uniform linear array (ULA), N_1 reflecting elements arranged in an ULA, N_2 reflecting elements arranged in an ULA and a single antenna, respectively. Due to the lack of an LoS propagation path between the BS and the user caused by severe obstructions, IRS1 and IRS2 are judiciously and constructively deployed on Building A near the BS and Building B near the user, respectively, to reap a cascaded BS-IRS1-IRS2-user link and improve the system performance. In addition, each IRS is joined to the BS by a dedicated transmission link to regulate signal reflection and exchange information.

Although the LoS path between the BS and the user is blocked, LoS paths can still be created in the channels between the BS and IRS1, between IRS1 and IRS2, and between IRS2 and the user by tactfully deploying the two IRSs in the wireless propagation environment. The three channels, therefore, can be modeled as Rician fading channels and expressed as follows [16, 17]:

$$\mathbf{H}_{1B} = \sqrt{\alpha_{1B}} \left(\sqrt{\frac{K_{1B}}{K_{1B} + 1}} \bar{\mathbf{H}}_{1B} + \sqrt{\frac{1}{K_{1B} + 1}} \tilde{\mathbf{H}}_{1B} \right) \tag{1}$$

$$\mathbf{H}_{21} = \sqrt{\alpha_{21}} \left(\sqrt{\frac{K_{21}}{K_{21} + 1}} \bar{\mathbf{H}}_{21} + \sqrt{\frac{1}{K_{21} + 1}} \tilde{\mathbf{H}}_{21} \right) \tag{2}$$

$$\mathbf{h}_{u2} = \sqrt{\alpha_{u2}} \left(\sqrt{\frac{K_{u2}}{K_{u2} + 1}} \bar{\mathbf{h}}_{u2} + \sqrt{\frac{1}{K_{u2} + 1}} \tilde{\mathbf{h}}_{u2} \right) \tag{3}$$

where $\mathbf{H}_{1B} \in \mathbb{C}^{N_1 \times M}$, $\mathbf{H}_{21} \in \mathbb{C}^{N_2 \times N_1}$, and $\mathbf{h}_{u2} \in \mathbb{C}^{N_2 \times 1}$ and α_{1B} , α_{21} , and α_{u2} denote the large-scale path losses of the BS-IRS1 link, IRS1-IRS2 link, and IRS2-user link, respectively. K_{1B} , K_{21} , and K_{u2} refer to the Rician factors of the BS-IRS1 link, IRS1-IRS2 link and IRS2-user link, respectively. $\bar{\mathbf{H}}_{1B} \in \mathbb{C}^{N_1 \times M}$, $\bar{\mathbf{H}}_{21} \in \mathbb{C}^{N_2 \times N_1}$, and $\bar{\mathbf{h}}_{u2} \in \mathbb{C}^{N_2 \times 1}$ represent the LoS components of their respective links. $\tilde{\mathbf{H}}_{1B} \in \mathbb{C}^{N_1 \times M}$, $\tilde{\mathbf{H}}_{21} \in \mathbb{C}^{N_2 \times N_1}$, and $\tilde{\mathbf{h}}_{u2} \in \mathbb{C}^{N_2 \times 1}$ depict the non-line-of-sight (NLoS) components of their respective links, whose elements are independently and identically distributed complex Gaussian random variables following the distribution of $CN(0,1)$.

The LoS components are delineated by the response of the ULA. The array response of an M -element ULA is as follows:

$$\mathbf{a}_M(\phi) = \left[1, e^{j2\pi \frac{d}{\lambda} \sin \phi}, \dots, e^{j2\pi \frac{d}{\lambda} (M-1) \sin \phi} \right]^T \tag{4}$$

where ϕ is the angle of arrival (AoA) or angle of departure (AoD) of a signal. In this case, the LoS component $\bar{\mathbf{H}}_{1B} \in \mathbb{C}^{N_1 \times M}$ can be defined as follows:

$$\bar{\mathbf{H}}_{1B} = \mathbf{a}_{N_1}(\phi_{\text{AoA}, 1B}) \mathbf{a}_M^H(\phi_{\text{AoD}, 1B}) \tag{5}$$

where $\phi_{\text{AoA}, 1B}$ is the AoA to ULA at IRS1 and $\phi_{\text{AoD}, 1B}$ is the AoD from the ULA at the BS. Similarly, the LoS components $\bar{\mathbf{H}}_{21} \in \mathbb{C}^{N_2 \times N_1}$ and $\bar{\mathbf{h}}_{u2} \in \mathbb{C}^{N_2 \times 1}$ are defined as follows:

$$\bar{\mathbf{H}}_{21} = \mathbf{a}_{N_2}(\phi_{\text{AoA}, 21}) \mathbf{a}_{N_1}^H(\phi_{\text{AoD}, 21}) \tag{6}$$

$$\bar{\mathbf{h}}_{u2} = \mathbf{a}_{N_2}(\phi_{\text{AoD}, u2}) \tag{7}$$

where $\phi_{\text{AoA}, 21}$, $\phi_{\text{AoD}, 21}$, and $\phi_{\text{AoD}, u2}$ are the AoA to ULA at IRS2, the AoD from the ULA at IRS1, and the AoD from the ULA at IRS2, respectively.

As the BS-IRS1-IRS2-user link is a cascaded channel, the received signal at the user can be stated as follows:

$$\mathbf{y} = (\mathbf{h}_{u2}^H \mathbf{\Theta}_2 \mathbf{H}_{21} \mathbf{\Theta}_1 \mathbf{H}_{1B}) \mathbf{w} \mathbf{s} + n \tag{8}$$

where $\mathbf{\Theta}_1 = \text{diag}(\eta_1^1 e^{j\theta_1^1}, \dots, \eta_{N_1}^1 e^{j\theta_{N_1}^1}) \in \mathbb{C}^{N_1 \times N_1}$ and $\mathbf{\Theta}_2 = \text{diag}(\eta_1^2 e^{j\theta_1^2}, \dots, \eta_{N_2}^2 e^{j\theta_{N_2}^2}) \in \mathbb{C}^{N_2 \times N_2}$ denote the reflection matrices of IRS1 and IRS2, respectively. $\eta_m^1 \in [0, 1]$ and $\eta_l^2 \in [0, 1]$ are amplitude reflection coefficients of IRS1 and IRS2, while $\theta_m^1 \in [0, 2\pi]$ and $\theta_l^2 \in [0, 2\pi]$ are the phase shifts introduced by IRS1 and IRS2. For simplicity, we will set $\eta_m^1 = \eta_l^2 = 1$ in the sequel to this paper. $\mathbf{w} \in \mathbb{C}^{M \times 1}$ and $s \sim \text{CN}(0, 1)$ indicate the transmit beamforming vector and the transmitted symbol, respectively. n is additive white Gaussian noise (AWGN) with zero mean and variance σ^2 . According to formula (8), we can obtain the signal power received at the user as follows:

$$\beta = |(\mathbf{h}_{u2}^H \mathbf{\Theta}_2 \mathbf{H}_{21} \mathbf{\Theta}_1 \mathbf{H}_{1B}) \mathbf{w}|^2 \tag{9}$$

2.2 Problem formulation

Assume that P is the maximum transmit power, $\boldsymbol{\theta}^1 = [\theta_1^1, \dots, \theta_{N_1}^1]^T$, and $\boldsymbol{\theta}^2 = [\theta_1^2, \dots, \theta_{N_2}^2]^T$. We aim to maximize the received signal power β by cooperatively optimizing the transmit beamforming \mathbf{w} and the phase shifts $\boldsymbol{\theta}^1$ and $\boldsymbol{\theta}^2$, subject to the maximum transmit power constraint at the BS. The corresponding optimization problem can be written as follows:

$$(P1) \quad \max_{\mathbf{w}, \boldsymbol{\theta}^1, \boldsymbol{\theta}^2} |(\mathbf{h}_{u2}^H \mathbf{\Theta}_2 \mathbf{H}_{21} \mathbf{\Theta}_1 \mathbf{H}_{1B}) \mathbf{w}|^2 \tag{10}$$

$$\text{s.t.} \quad \|\mathbf{w}\|^2 \leq P, \tag{11}$$

$$0 \leq \theta_m^1 \leq 2\pi, \forall m = 1, \dots, N_1, \tag{12}$$

$$0 \leq \theta_l^2 \leq 2\pi, \forall l = 1, \dots, N_2. \tag{13}$$

We postulate that CSI is always acquirable. Therefore, for any specific $\boldsymbol{\theta}^1$ and $\boldsymbol{\theta}^2$, it is not difficult to find that the maximum-ratio transmission (MRT) is the optimal transmit beamforming method for the optimization problem (P1) [18], i.e., $\mathbf{w}^* = \sqrt{P} \frac{(\mathbf{h}_{u2}^H \mathbf{\Theta}_2 \mathbf{H}_{21} \mathbf{\Theta}_1 \mathbf{H}_{1B})^H}{\|(\mathbf{h}_{u2}^H \mathbf{\Theta}_2 \mathbf{H}_{21} \mathbf{\Theta}_1 \mathbf{H}_{1B})\|} \triangleq \mathbf{w}_{\text{MRT}}$. By substituting \mathbf{w}^* into formula (10), (P1) can be transformed to the following equivalent problem:

$$\frac{(\mathbf{h}_{u2}^H \mathbf{\Theta}_2 \mathbf{H}_{21} \mathbf{\Theta}_1 \mathbf{H}_{1B})^H}{\|(\mathbf{h}_{u2}^H \mathbf{\Theta}_2 \mathbf{H}_{21} \mathbf{\Theta}_1 \mathbf{H}_{1B})\|} \triangleq \mathbf{w}_{\text{MRT}}. \tag{10}$$

By substituting \mathbf{w}^* into formula (10), (P1) can be transformed to the following equivalent problem:

$$(P2) \quad \max_{\boldsymbol{\theta}^1, \boldsymbol{\theta}^2} \left\| (\mathbf{h}_{u2}^H \mathbf{\Theta}_2 \mathbf{H}_{21} \mathbf{\Theta}_1 \mathbf{H}_{1B}) \right\|^2 \tag{14}$$

$$\text{s.t.} \quad 0 \leq \theta_m^1 \leq 2\pi, \forall m = 1, \dots, N_1, \tag{15}$$

$$0 \leq \theta_l^2 \leq 2\pi, \forall l = 1, \dots, N_2. \tag{16}$$

Although constraints (15) and (16) are convex, problem (P2) remains a non-convex optimization problem because of the non-concave objective function with respect to θ^1 and θ^2 . In practice, there is no standard solution to such a non-convex optimization problem. Accordingly, we propose to resort to the PSO algorithm to optimize problem P2, which will be analyzed in the next section.

3 Method

In this section, we first describe the fundamental principle of PSO and then capitalize on the PSO algorithm to address the proposed non-convex optimization problem.

3.1 Particle swarm optimization

As a stochastic global optimization solution, PSO has been proven to be robust and fast in solving non-linear, non-differentiable, continuous variables, and multimodal problems [19, 20]. PSO is derived from real life (i.e., a flock of birds or a school of fish) and swarming theory. As indicated by the name, PSO consists of a swarm of particles, similar to a group of flying birds. Here, each particle is a candidate or potential solution to the optimization problem. During the optimization process performed by the PSO algorithm, suppose that there is a cluster of particles randomly distributed in a multidimensional space, and each particle has its own fitness value determined by its spatial position and velocity. Then, each particle hunts for the optimal position in the searching space based on its current position. Each particle, in every iteration, abides by the following two “extremums” to adjust its position and velocity. One extremum is the individual optimal position $pbest$, which is searched by itself; based on this position, the individual best fitness value can be determined. The other is the global optimal position $gbest$, which is searched by the whole swarm; this position can be used to calculate the global best fitness value.

Assume that $x_i(i = 1, 2, \dots, D)$ are the initial positions of the optimization problem (with D as the swarm size). Each particle is updated according to the following equations:

$$v_i^{t+1} = wv_i^t + c_1r_1(pbest_i - x_i^t) + c_2r_2(gbest_i - x_i^t) \quad (17)$$

$$x_i^{t+1} = x_i^t + v_i^{t+1} \quad (18)$$

where x_i and v_i represent the position and velocity respectively, w is the inertia weight, c_1 and c_2 are the learning factors, and r_1 and r_2 are two random numbers between 0 and 1. Note that the velocity $v_i \in [-v_{\max}, v_{\max}]$ is generally bounded between the maximum v_{\max} and the minimum $-v_{\max}$. It is worth mentioning that if the velocity is too high, the best solution may be missed, while if the velocity is too low, there may be insufficient searching space.

3.2 Optimization procedure

According to the abovementioned principle, the optimization procedure for problem (P2) based on PSO is as follows:

Step 1: Initialize the swarm size D , the maximum number of iterations T_{max} , the particle position $x_i \in [0, 2\pi]$, the velocity $v_i \in [-v_{\max}, v_{\max}]$, w , $c1$, $c2$ and $r1$, $r2$.

Step 2: The fitness value of each particle is obtained according to formula (14).

Step 3: For each particle, when the fitness value at the current position is greater than the previous best fitness value, set the current position as *pbest*.

Step 4: For each particle, when its best fitness value is greater than the global best fitness value of the swarm, set the best fitness value of this particle as the global best fitness value, and set its corresponding position as *gbest*.

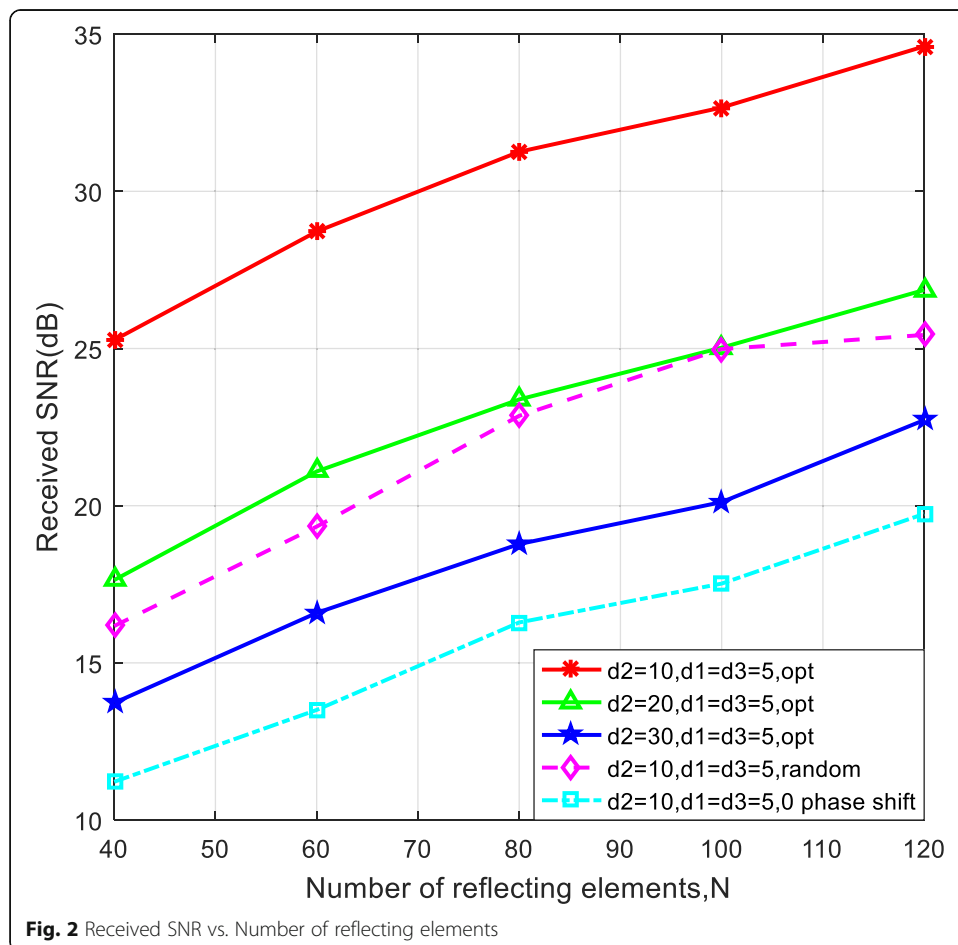
Step 5: Adjust the velocity and position of each particle based on formulas (17) and (18), respectively.

Step 6: If the maximum number of iterations is reached, stop iterating, save, and output the results, or return to Step 2.

In this paper, the main parameter set for PSO includes $D = 30$, $T_{\max} = 100$, $v_{\max} = 0.1$, $w = 0.1$, and $r_1 = r_2 = 0.5$. These parameters are chosen based on the results of many simulations.

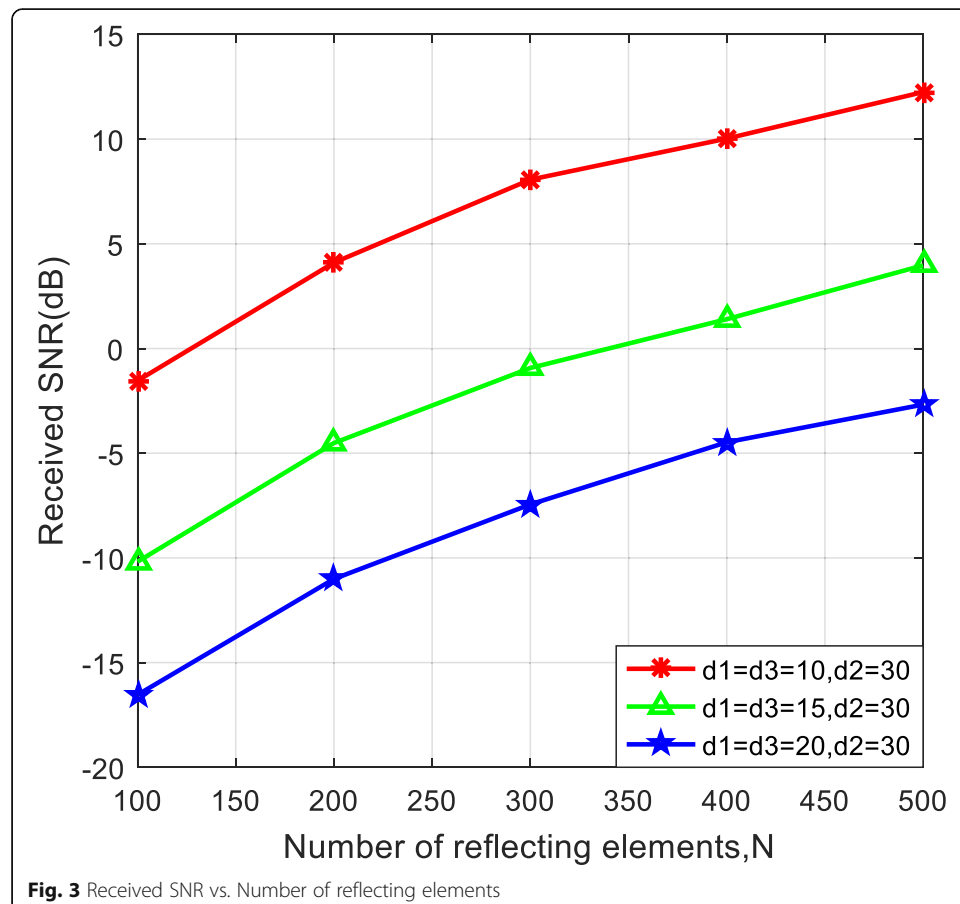
4 Results and discussion

All results in this section are attained by averaging over 1000 independent trials. The simulation layout is shown in Fig. 1, where d_1 , d_2 , and d_3 are the straight-line distances between the BS and IRS1, IRS1 and IRS2, and IRS2 and the user, respectively. The simulation parameters are as follows: $M = 9$, $N_1 = N_2 = N$, $\sigma^2 = -110$ dBm, $P = 11$ dBm and $K_{1B} = K_{21} = K_{u2} = 10$. We choose different d_1 , d_2 , d_3 , and N to verify the performance of the double-IRS-aided wireless network. The large-scale path loss could



be calculated by $\alpha = \frac{1}{1000d^{ple}}$, in which d denotes the corresponding link distance and ple represents the associated path-loss exponent. Angles of the LoS components in the respective channels is randomly set within $[0, 2\pi]$. When d_1 , d_2 , and d_3 are less than 10 m, the corresponding path-loss exponents of α_{1B} , α_{21} , and α_{u2} are 2, while when d_1 , d_2 , and d_3 are equal to or greater than 10 m, the associated path-loss exponents of α_{1B} , α_{21} , and α_{u2} are 2.5.

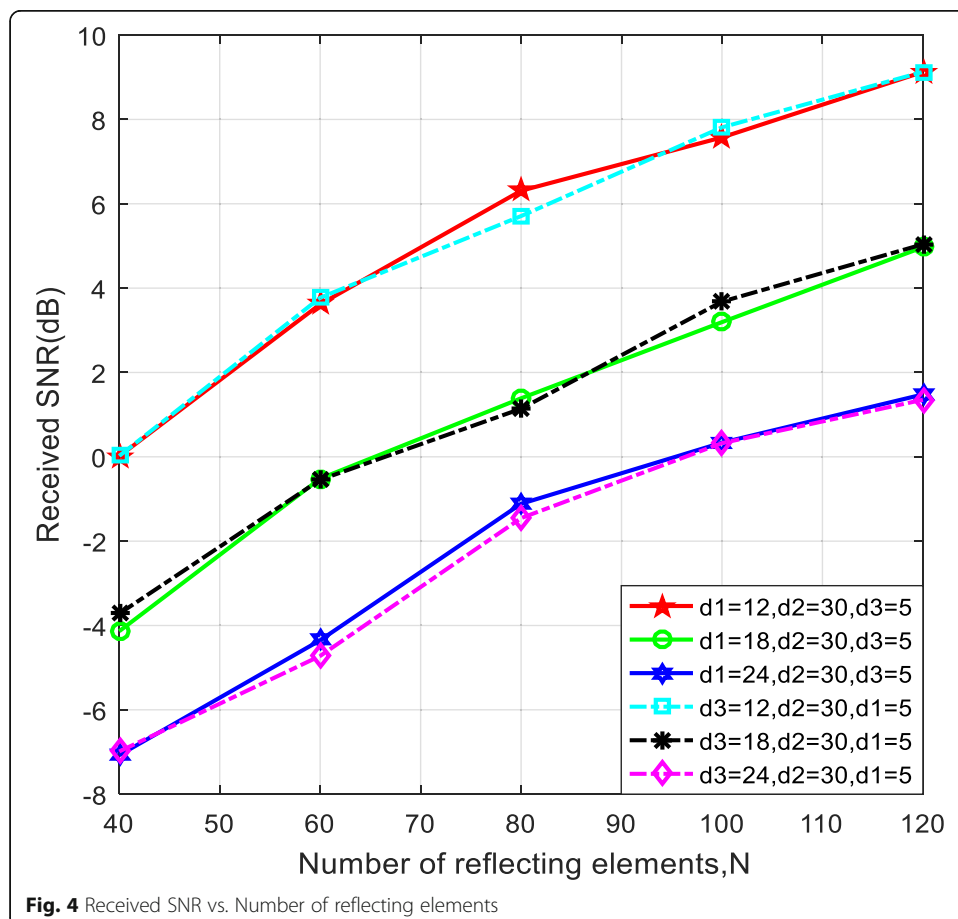
In Fig. 2, we assume that d_1 and d_3 are both equal to 5 m. In this context, to compare received SNRs with different distances between IRS1 and IRS2, we select three different distances of d_2 , which are 10 m, 20 m, and 30 m. We can observe in Fig. 2 that when IRS1 and IRS2 are composed of fewer reflecting elements, the received SNRs at the user are large and guaranteed, despite there being no direct LoS path available from the transmitter to the receiver. Nevertheless, as the distances from IRS1 to IRS2 are increased, the received SNRs decrease. The reason is that the signals are further attenuated with increasing distance. In the meantime, with $d_1 = d_3 = 5$ m and $d_2 = 10$ m, we also acquire different SNRs when the phase shifts on IRS1 and IRS2 are 0, random, and optimized, respectively. It is obvious that in Fig. 2, the received SNRs rise significantly after the phase shifts are optimized. Accordingly, the curves in Fig. 2 indicate that it is feasible to deploy two distributed IRSs in the immediate vicinity of the BS and the user to create a cascaded BS-IRS1-IRS2-user channel and ensure system performance. However, it remains unknown whether the received SNRs at the user



could be accepted and guaranteed when the IRS1 and IRS2 are deployed far from the BS and the user. Hence, this must be verified via simulation.

Considering that longer traveling distances of signals will increase signal attenuation, we select the two IRSs composed of more reflecting elements to maximally offset attenuation. We fix $d_2 = 30$ m first and then set $d_1 = d_3 = 10$ m, 15 m, and 20 m, as displayed in Fig. 3. When d_1 and d_3 are too large, the received SNRs cannot be accepted despite more reflecting elements on IRS1 and IRS2. Specifically, when $d_1 = d_3 = 10$ m and $d_2 = 30$ m, the received SNRs rise with an increasing number of reflecting elements and most of the SNRs are greater than 0 dB. However, when $d_1 = d_3 = 20$ m and $d_2 = 30$ m, the received SNRs remain less than 0 dB although the number of reflecting elements has reached 500. Fortunately, according to Fig. 3, as long as the number of reflecting elements on the two IRSs continues to rise, the SNRs will be greater than 0 dB again; thus, the system performance can be guaranteed. Consequently, it is suggested that farther transmission of signals is at the expense of significantly increasing the number of reflecting elements on an IRS.

In addition to the above two situations, we simulate the system performance when IRS1 and IRS2 are fixed, while the BS and user exchange positions. Specifically, when d_2 is fixed at 30 m, the received SNRs under the conditions of $d_1 = 12$ m, 18 m, and 24 m, while $d_3 = 5$ m, are nearly equal to the SNRs when $d_3 = 12$ m, 18 m, and 24 m, while $d_1 = 5$ m. As we can see from Fig. 4, the maximum differences between the SNRs



when the user and base station exchange positions are no more than 1 dB, and they are sometimes equal.

5 Conclusion

In this article, we have investigated how to utilize two IRSs to improve the wireless communication system performance when there is no direct LoS path between the transmitter and the receiver. To be specific, we deploy two distributed IRSs (IRS1 and IRS2) in the vicinity of the BS and user to achieve a cascaded BS-IRS1-IRS2-user channel. By cooperatively optimizing the transmit and passive beamforming on the two IRSs based on the PSO algorithm, the received SNRs at the user are derived. The simulation results imply that with a short distance from the BS to the user, the obtainable SNRs at the user are large, even if each IRS consists of fewer reflecting elements. The results also indicate that it is essential to significantly increase the number of reflecting elements on the IRS to achieve an accepted SNR when there is a long distance between the BS and the user. In the meantime, we unexpectedly find that when the positions of the two IRSs are fixed, the obtainable SNRs are nearly equal when exchanging the positions of the BS and the user. In summary, it is feasible to improve the quality of wireless communication via double reflection links composed of two IRSs, which undoubtedly can provide a powerful solution for achieving seamless global coverage in future 6G wireless communications.

Abbreviations

IRS: Intelligent reflecting surface; BS: Base station; PSO: Particle swarm optimization; LoS: Line-of-sight; SNR: Signal-to-noise ratio; CSI: Channel state information; RIS: Reconfigurable intelligent surface; LIS: Large intelligent surface; MISO: Multiple-input-single-out; ULA: Uniform linear array; NLoS: Non-line-of-sight; AoA: Angle of arrival; AoD: Angle of departure; AWGN: Additive white Gaussian noise; MRT: Maximum-ratio transmission

Acknowledgements

The authors would like to express our gratitude to the anonymous reviewers for their valuable comments and suggestions that helped improve the quality of the manuscript.

Authors' contributions

All authors have contributed equally. All authors have read and approved the final manuscript.

Funding

This work was supported by the Postgraduate Research & Practice Innovation Program of Jiangsu Province of China Grant Number KYCX20_0719.

Availability of data and materials

Please contact the corresponding author for data requests.

Declarations

Competing interests

The authors declare that they have no competing interests.

Received: 14 May 2021 Accepted: 26 July 2021

Published online: 13 August 2021

References

1. S. Gong, X. Lu, D.T. Hoang, D. Niyato, L. Shu, D.I. Kim, Y.C. Liang, Toward smart wireless communications via intelligent reflecting surfaces: a contemporary survey. *IEEE Communications Surveys & Tutorials* **22**(4), 2283–2314 (2020)
2. Q. Wu, S. Zhang, B. Zheng, C. You, R. Zhang, Intelligent reflecting surface aided wireless communications: a tutorial. *IEEE Trans. Commun.* **69**(5), 3313–3351 (2021)
3. C. Huang, A. Zappone, G.C. Alexandropoulos, M. Debbah, C. Yuen, Reconfigurable intelligent surfaces for energy efficiency in wireless communication. *IEEE Transactions Wireless Communications* **18**(8), 4157–5170 (2019)
4. C Pan, H Ren, K Wang, J F Kolb, L Hanzo, Reconfigurable intelligent surfaces for 6G and beyond: principles, applications, and research directions, <https://arxiv.org/pdf/2011.04300v4.pdf>. Accessed 2 May 2021.
5. W. Saad, M. Bennis, M. Chen, A vision of 6G wireless systems: applications, trends, technologies, and open research problems. *IEEE Netw.*, 134–142 (2020)

6. C. Pan, H. Ren, K. Wang, M. Elkashlan, L. Hanzo, Intelligent reflecting surface aided MIMO broadcasting for simultaneous wireless information and power transfer. *IEEE Journal on Selected Areas in Communications* **38**(8), 1719–1314 (2020)
7. X. Yu, D. Xu, R. Schober, Robust and secure wireless communications via intelligent reflecting surfaces. *IEEE Journal on Selected Areas in Communications* **38**(11), 2637–2652 (2020)
8. Z. Peng, Z. Zhang, C. Pan, L. Li, A.L. Swindlehurst, Multiuser Full-Duplex Two-Way Communications via Intelligent Reflecting Surface. *IEEE Trans. Signal Process.* **69**, 837–851 (2021)
9. S. Lin, B. Zheng, G.C. Alexandropoulos, M. Wen, S. Mumtaz, Adaptive transmission for reconfigurable intelligent surface-assisted OFDM wireless communications. *IEEE Journal on Selected Areas in Communications* **38**(11), 2653–2665 (2020)
10. G. Zhou, C. Pan, H. Ren, K. Wang, A. Nallanathan, A framework of robust transmission design for IRS-aided MISO communications with imperfect cascaded channels. *IEEE Trans. Signal Process.* **68**, 5092–5106 (2020)
11. W. Shi, J. Li, G. Xia, Y. Wang, X. Zhou, Y. Zhang, F. Shu, Secure multigroup multicast communication systems via intelligent reflecting surface. *China Communications* **18**(3), 39–51 (2021)
12. W. Shi, X. Zhou, L. Jia, Y. Wu, F. Shu, J. Wang, Enhanced secure wireless information and power transfer via intelligent reflecting surface. *IEEE Commun. Lett.* **25**(4), 1084–1088 (2021)
13. X. Zhou, S. Yan, Q. Wu, F. Shu, DWK Ng, Intelligent reflecting surface (IRS)-aided covert wireless communication with delay constraint, <https://arxiv.org/pdf/2011.03726.pdf>. Accessed 7 Nov 2020.
14. F. Shu, J. Li, M. Huang, W. Shi, Y. Teng, J. Li, Y. Wu, J. Wang, Enhanced secrecy rate maximization for directional modulation networks via IRS, <https://arxiv.org/pdf/2008.05067v1.pdf>. Accessed 12 Aug 2020.
15. F. Shu, X. Jiang, W. Cai, W. Shi, M. Huang, J. Wang, X. You, Beamforming and Transmit Power Design for Intelligent Reconfigurable Surface-aided Secure Spatial Modulation, <https://arxiv.org/pdf/2106.03616.pdf>. Accessed 7 Jun 2021.
16. Y. Han, W. Tang, S. Jin, C. Wen, X. Ma, Large intelligent surface-assisted wireless communication exploiting statistical CSI. *IEEE Trans. Veh. Technol.* **68**(8), 8238–8243 (2019)
17. K. Zhi, C. Pan, H. Ren, K. Wang, Power scaling law analysis and phase shift optimization of RIS-aided massive MIMO systems with statistical CSI, <https://arxiv.org/pdf/2010.13525v4.pdf>. Accessed 20 Jan 2021.
18. T.K.Y. Lo, Maximum ratio transmission. *IEEE Trans. Commun.* **47**(10), 1458–1461 (1999)
19. J. Kenney, R. Eberhart, *Proceedings of ICNN'95-International Conference on Neural Networks. Particle Swarm Optimization* (IEEE, Perth, 1995), pp. 1942–1948
20. Y. Shi, R. Eberhart, *Proceedings IEEE International Conference on Evolutionary Computation. A modified particle swarm optimizer* (IEEE, Anchorage, 1998), pp. 69–73

Publisher's Note

Springer Nature remains neutral with regard to jurisdictional claims in published maps and institutional affiliations.

Submit your manuscript to a SpringerOpen[®] journal and benefit from:

- Convenient online submission
- Rigorous peer review
- Open access: articles freely available online
- High visibility within the field
- Retaining the copyright to your article

Submit your next manuscript at ► [springeropen.com](https://www.springeropen.com)
